

Independently Tuning Elastomer Softness and Firmness by Incorporating Side Chain Mixtures into Bottlebrush Network Strands

Andrew N. Keith, Charles Clair, Abdelaziz Lallam, Egor A. Bersenev, Dimitri A. Ivanov, Yuan Tian, Andrey V. Dobrynin,* and Sergei S. Sheiko*

Cite This: *Macromolecules* 2020, 53, 9306–9312

Read Online

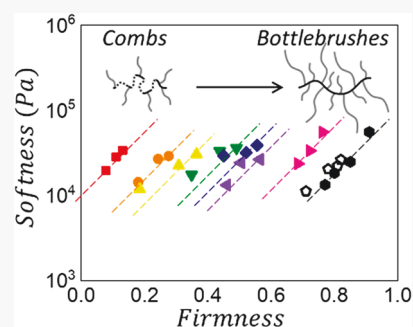
ACCESS |

Metrics & More

Article Recommendations

Supporting Information

ABSTRACT: Softness and firmness are opposing traits that synergistically define the elastic response of biological systems. Currently, no single class of synthetic materials including elastomers and gels provides independent control of these mechanical characteristics, particularly without altering chemical composition. To address this challenge, we explore a hierarchical bottom-up approach via architectural modulation of bottlebrush mesoblocks followed by their self-assembly into linear–brush–linear triblock copolymer networks. By judiciously incorporating side chains of different lengths, we seamlessly demonstrate full control over elastomer firmness at a fixed Young's modulus, thus bypassing the infinitely laborious synthesis of targeted side chain lengths. This industrially scalable iteration upon the design-by-architecture approach to network construction delivers thermoplastic elastomers with unprecedented softness–firmness combinations desired in soft robotics, flexible electronics, and biomedical devices.



INTRODUCTION

Stress–strain responses of elastic materials can be expressed by two distinct mechanical characteristics: (i) Young's modulus (E_0), which defines material stiffness (or softness) at small strains, and (ii) firmness (β), which characterizes stiffening during deformation (Figure 1A).^{1,2} Although firmness is colloquially used in the English language as a synonym of stiffness, various sectors in industry use this mechanical label to characterize the resistance to deformation of *soft* systems such as mattresses,³ food,⁴ and biological tissues.⁵ In other words, *firmness is not stiffness*. This distinction is observable in stress–strain curves of representative classes of soft materials (Figure 1A). Specifically, tissues and gels may show similar softness with $E_0 \sim 10$ kPa, but their stress–strain curves rapidly diverge during deformation.⁶ This intense strain stiffening represents one of nature's defense mechanisms preventing accidental rupture and uncontrolled sagging of living tissues.

While the molecular mechanism of biological firmness is complex and viscoelastic in nature,^{7,8} the structural interpretation of polymer network's elastic response is straightforward.^{1,9} The nonlinear modulus increase results from finite extensibility of network strands defined by the initial mean-square end-to-end distance between cross-links ($\langle R_{in}^2 \rangle$) to the square of the strand contour length R_{max}^2 as $\beta = \langle R_{in}^2 \rangle / (R_{max}^2)$, which is within interval $0 < \beta < 1$ (Figure 1A). Networks with flexible strands ($R_{in} \ll R_{max}$) display weak strain stiffening with $\beta \cong 0.01$ – 0.1 , while semiflexible networks ($R_{in} \sim R_{max}$) are characterized by $\beta \approx 0.1$ – 1 .

For various elastic systems, the softness (E_0) and firmness (β) are readily quantified by fitting experimental stress–strain curves (Figure 1A) with the following equation of state:⁹

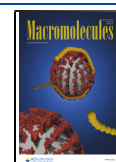
$$\sigma_{true}(\lambda) = \frac{E}{9}(\lambda^2 - \lambda^{-1}) \left[1 + 2 \left(1 - \frac{\beta(\lambda^2 + 2\lambda^{-1})}{3} \right)^{-2} \right] \quad (1)$$

where E is the structural modulus related to cross-link density. Jointly, E and β define the Young's modulus $E_0 = E(1 + 2(1 - \beta)^{-2})/3$, which corresponds to the stress–strain slope at $\lambda \rightarrow 0$. By plotting the extracted parameters of various elastic systems on an $[E_0, \beta]$ map, we expose a remarkable absence of independent control over E_0 and β to cover the entire map (Figure 1B). For instance, conventional elastomers with flexible strands exhibit low firmness $\beta < 0.01$ and relatively high modulus $E_0 > 10^5$ Pa as they are architecturally limited by chain entanglements.^{10,11} In polymer gels, swelling with solvent enables decoupling the elastic features which leads to both dilution of network strands and their extension toward lower E_0 and higher β , respectively. However, gels are also limited by strand entanglements bounding firmness to $\beta < 0.2$ (Figure 1B).^{6,11} Although significant progress has been achieved with

Received: July 24, 2020

Revised: October 5, 2020

Published: October 23, 2020



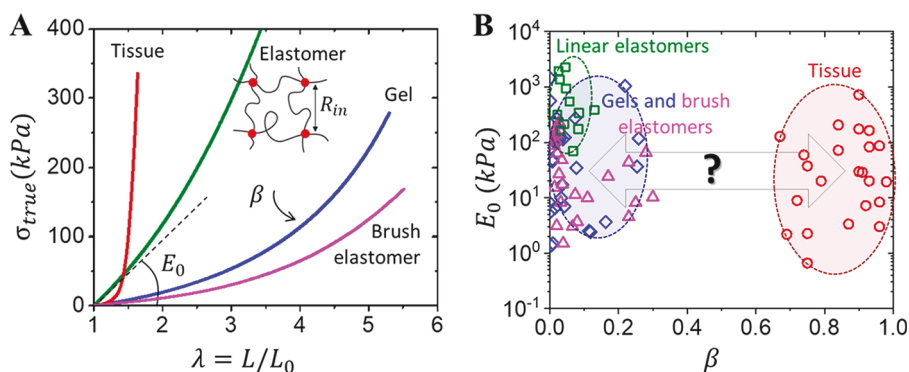


Figure 1. Elastic landscape. (A) Representative stress–elongation curves of various elastic materials with similar softness ($E_0 = 20$ kPa) but vastly distinct firmness: PAM gel (blue),⁶ a covalently cross-linked brush elastomer (magenta, $n_x = 600$, $n_{sc} = 14$, and $n_g = 2$),¹⁷ and fetal membrane tissue (red).⁶ Linear elastomers (green) cannot reach tissue relevant softness due to linear entanglements.¹⁰ (B) $[E_0, \beta]$ map depicting distinct classes of materials including linear elastomers (\square),^{1,10,11} gels (\diamond),⁶ brushlike elastomers (Δ),^{17,18} and tissue (\circ).⁶

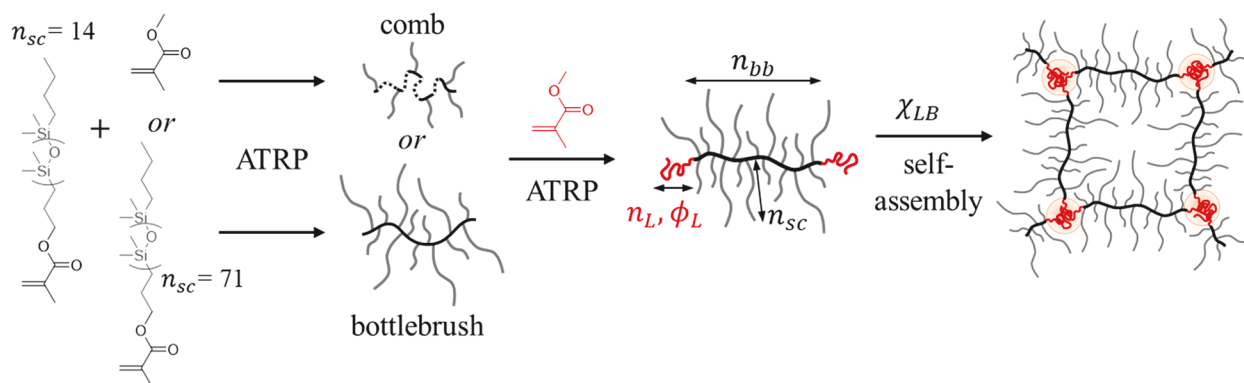


Figure 2. Linear–bottlebrush–linear (LBL) plastomer synthetic route. Copolymerization of two PDMS-MA macromonomers with $n_{sc} = 14$ and 71 and MMA monomer enables accurately tuning the average $\langle n_{sc} \rangle$ of the brush block within LBL macromolecules that subsequently self-assemble into physical networks.

more complex architectures such as dual network gels¹² and sacrificial cross-links,¹³ these systems face similar limitations ($\beta < 0.4$) and typically possess high E_0 due to dense cross-linking.⁶ On the opposite end of the $[E_0, \beta]$ map, we realize biology's unrivaled mechanics demonstrating broad softness $10^2 < E_0 < 10^6$ and firmness $\beta > 0.7$ (Figure 1B).^{6,14–16} Yet, from the $[E_0, \beta]$ map, it is apparent that neither nature nor current synthetic strategies contain the tools to successfully decouple E_0 and β over the entire elastic landscape. Therefore, the goal of this study is to develop a materials design platform that broadly and independently varies firmness and softness. Specifically, we aim to demonstrate continuous firmness enhancement from $\beta \sim 0 \rightarrow 1$ at constant Young's modulus E_0 .

In this regard, brushlike polymers^{6,17–27} offer a promising path forward by exploiting the oxymoronic duality of side chains as mechanical softeners and stiffeners. At a given network strand length, introducing side chains has two concurrent effects: (i) increased strand volume resulting in decreased E_0 and (ii) strand extension resulting in enhanced β . Two classes of brush elastomers mimic the mechanical properties of gels and tissues: (i) covalently cross-linked elastomers^{17,18} and (ii) physically cross-linked plastomers obtained by self-assembly of linear–brush–linear (LBL) triblock copolymers.^{6,27} The elastic footprint of covalently cross-linked brushlike elastomers is strikingly similar to those of gels with limited firmness of $\beta < 0.3$ (Figure 1B).^{17,18} Therefore, we focus on plastomers, which afford higher firmness due to the strong segregation of both the compositionally and architecturally distinct blocks.^{6,27,28} In previous

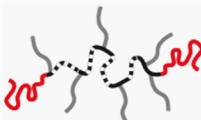
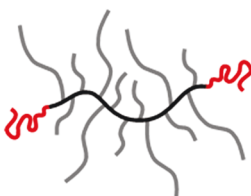
studies, varying brush block length and linear block length led to an undesirable simultaneous increase of E_0 and β .²⁷ To enable independent control over E_0 and β , we employed longer side chains, which excel at respectively augmenting strand volume and stiffness.⁶ Although these materials successfully decouple E_0 and β as the first elastomers to replicate the unprecedented softness–firmness combination of tissue, they encompassed a narrow elastic range. Therefore, broadly augmenting both side chain length and linear block volume fraction paves a pathway to covering the entire landscape within a single copolymer platform as investigated by this report.

RESULTS AND DISCUSSION

One of the most efficient ways to vary the average degree of polymerization (DP) of side chains, $\langle n_{sc} \rangle$, is through copolymerization of small and large (macro)monomers at controlled molar fractions (Figure 2). This side chain mixing approach bypasses the commercial limitations found in previous brush systems with monodisperse side chains^{6,27} by enabling broad and continuous tuning of $\langle n_{sc} \rangle$ with minimum synthetic efforts while delivering elastomers with well-defined mechanical properties.

To validate this approach, we have synthesized nine series of LBL triblock copolymers with increasing $\langle n_{sc} \rangle$ (Table 1) via atom transfer radical polymerization (ATRP) consistent with previous efforts to maximize conversion and yield.²⁹ In the comb group (series 1–3), $\langle n_{sc} \rangle$ was controlled by the copolymeriza-

Table 1. Molecular Parameters of LBL Block Copolymers

Sample	m_1/m_2^c	$\langle n_{sc} \rangle^d$	n_{bb}^e	n_L^f	ϕ_L^g	Schematics
Series 1 ^a MMA/S14 50/50	52/48	7.5	336	78	0.069	 Combs
		7.5	336	102	0.089	
		7.5	336	119	0.102	
Series 2 ^a MMA/S14 25/75	27/73	10.8	196	34	0.038	
		10.8	196	58	0.062	
		10.8	196	64	0.068	
Series 3 ^a MMA/S14 10/90	11/89	12.9	197	29	0.027	
		12.9	197	52	0.047	
		12.9	197	76	0.067	
Series 4 ^b S14/S71 100/0	100/0	14.4	363	57	0.026	 Bottlebrushes
		14.4	363	116	0.053	
		14.4	363	168	0.077	
Series 5 ^b S14/S71 75/25	84/16	23.6	285	88	0.026	
		23.6	285	123	0.036	
		23.6	285	201	0.059	
Series 6 ^b S14/S71 50/50	66/34	33.8	249	62	0.014	
		33.8	249	106	0.024	
		33.8	249	133	0.029	
Series 7 ^b S14/S71 25/75	42/58	47.1	308	187	0.025	
		47.1	308	261	0.035	
		47.1	308	430	0.058	
Series 8 ^b S14/S71 0/100	0/100	71.2	447	288	0.020	
		71.2	447	604	0.041	
		71.2	447	772	0.052	
		71.2	447	894	0.060	
Series 9 ^b S14/S71 0/100	0/100	71.2	292	144	0.021	
		71.2	292	263	0.038	
		71.2	292	468	0.067	
		71.2	292	696	0.099	

^{a,b}Brush blocks copolymerized with molar fractions MMA and PDMS-MA $n_{sc} = 14$ (S14) macromonomers and brush blocks copolymerized with molar fractions of PDMS-MA $n_{sc} = 14$ (S14) and $n_{sc} = 71$ (S71) macromonomers. Both the n_{sc} of S14 and S71 are calculated from ^1H NMR (Figure S1). ^cFinal copolymer molar fractions measured by ^1H NMR (Figures S2–S10) where m_1 and m_2 are molar fractions of the respective (macro)monomers. ^dNumber-average degree polymerization of side chains calculated as $\langle n_{sc} \rangle = m_1 n_{sc,1} + m_2 n_{sc,2}$. ^eNumber-average degree polymerization of brush backbones. ^{f,g}Degree polymerization and volume fraction of linear MMA blocks as determined from ^1H NMR (Figures S11–S18) where $\rho_{\text{PMMA}} = 1.15$ g/mL and $\rho_{\text{PDMS}} = 0.96$ g/mL.

tion of poly(dimethylsiloxane–methacrylate) (PDMS–MA) macromonomer (S14, $n_{sc} = 14$) and methyl methacrylate (MMA) monomer (Figure 2). In the bottlebrush group (series 4–9), $\langle n_{sc} \rangle$ was varied by randomly copolymerizing (PDMS–MA) macromonomers with $n_{sc} = 14$ (S14) and 71 (S71) (Figure 2) while keeping the grafting density of side chains on the backbone constant ($n_g = 1$). Each series has slight brush block DP variation ($n_{bb} \approx 200$ –350) but contains triblocks with different volume fractions (ϕ_L) of PMMA chosen as the linear block due to strong PDMS–PMMA microphase separation^{6,27,28} (for complete data sets see Tables S1 and S2 and Figures S1–S18), although additional L-block chemistry should be investigated in future work. Side chain inclusion during polymerization was monitored by time-resolved ^1H NMR showing an anticipated enrichment of shorter macromonomers at initial degrees of conversion ($\sim 10\%$) but yield brush blocks within stoichiometric expectations ($<15\%$) (Figures S1–S10 and Tables S3 and S4). The resulting bottlebrush dimensions and side chain homogeneity along the backbone were verified by

atomic force microscopy (AFM) and ultrasmall-angle X-ray (USAXS) (Figure 3). Molecular imaging of dense monolayers by AFM reveals evenly spaced wormlike macromolecules with no signs of bimodality (Figure 3A). The spacing increases linearly with side chain weight-average $\langle n_{sc,w} \rangle$ (Figure 3B), which is consistent with the thermodynamically preferred adsorption of longer side chains to substrates.³⁰ Likewise, USAXS measurements of bulk LBL plastomers and B block melts show a consistent monomodal shift of a characteristic scattering peak around $q \approx 1$ nm^{−1} (Figure 3C), which is typically oversimplified as a backbone–backbone correlation or brush diameter.^{28,31–33} The resulting spacing $\xi = 2\pi/q$ scales with $\langle n_{sc} \rangle$ as $\xi \sim \langle n_{sc} \rangle^{0.41 \pm 0.01}$ (Figure 3D) and is consistent with recent small-angle neutron scattering ($\xi \sim n_{sc}^{0.40 \pm 0.04}$),³³ computer simulations ($\xi \sim n_{sc}^{0.39 \pm 0.01}$), and theoretical studies ($\xi \sim n_{sc}^{3/8}$).³⁴ The last highlights the complex physical origin of ξ due to coupled density fluctuations from both backbone monomers and side chains constrained by melt incompressibility.³⁴ The theory considers dependence of n_{sc} on the effective

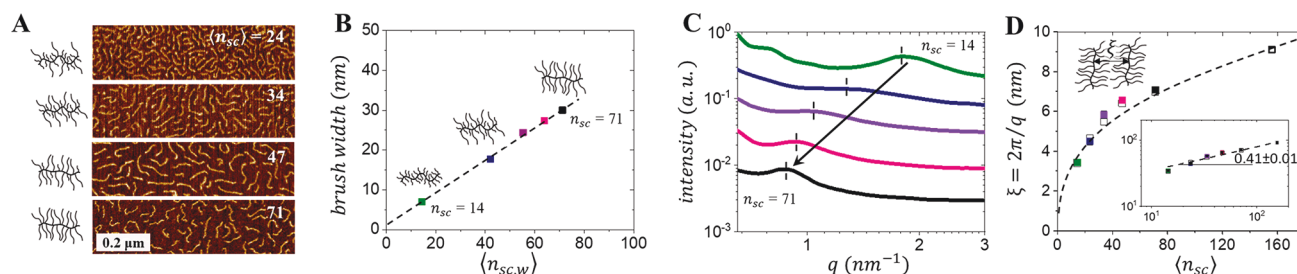


Figure 3. LBL Characterization. (A) Atomic force microscopy micrographs of Langmuir–Blodgett monolayers of brush blocks show increased interbrush distance with increasing fractions of long side chains ($n_{sc} = 71$). Unlike bottlebrushes with homogeneous side chains,³⁵ preferential absorption of larger side chains onto the substrate in mixed brushes dominates backbone extension resulting in a weak increase of the apparent persistence length with $\langle n_{sc} \rangle$. (B) Interbrush distance as determined by AFM (Figure S19 and Table S5) increases linearly with weight-average $\langle n_{sc,w} \rangle$. (C) Brush scattering peak, as determined in recent literature,^{6,28} consistently shifts to lower magnitudes of the scattering wavevector q with increasing number-average side chain length $\langle n_{sc} \rangle$. The peak at 0.8 nm^{-1} corresponds to the last visible ripple of the polydisperse sphere form factor. (D) Brush scattering distance peak position ($\xi = 2\pi/q$) increases with $\langle n_{sc} \rangle$ as $\xi \sim \langle n_{sc} \rangle^{0.41}$ (inset, in angstroms), which is consistent with theoretically predicted scaling behavior $\xi \sim n_{sc}^{3/8}$.²⁵ The dashed line corresponds to a linear fit with $\xi = 0.5 + 1.2n_{sc}^{0.41}$. The solid and open symbols correspond to LBL elastomers and melts of brush blocks, respectively, including a melt of PDMS bottlebrushes with long side chains ($n_{sc} = 156$). Importantly, upon background subtraction the brush scattering peak reveals its second order which indicates that packing of the bottlebrush segments is characterized by long-range order (cf. Figures S24 and S25).

bottlebrush block Kuhn length as $b_K \sim n_{sc}^{1/2}$, resulting in $\xi \sim n_{sc}^{1/4} b_K^{1/4} \sim n_{sc}^{3/8}$, which is weaker than the distance between brush backbones $\xi \sim n_{sc}^{1/2}$. A weaker power law may be also explained by an increased distance between neighboring side chains along the backbone with longer n_{sc} as $l \sim n_{sc}^\alpha$, which would lead to $\xi \sim n_{sc}^{1/2}/l = n_{sc}^{1/2-\alpha}$.

For each sample in all nine series, we measured their stress–elongation response (Figure S20) and characterized their E_0 and β (Figure S20 and Tables S1 and S2). Two sets of representative curves with either similar E_0 and varied β (Figure 4A), or vice versa (Figure 4B), demonstrate the unprecedented ability of the LBL plastomer platform to cover the $[E_0, \beta]$ landscape. In Figure 4A, the curves show significant variation of strain stiffening (β) at nearly constant slope at $\lambda \rightarrow 1$ (E_0) with larger $\langle n_{sc} \rangle$. In Figure 4B, increasing E_0 at nearly constant β was achieved by concomitantly varying $\langle n_{sc} \rangle$ and volume fraction of the linear block (ϕ_L) as indicated. The corresponding E_0 and β values were extracted by fitting the stress–strain curves with eq 1 with an $[E_0, \beta]$ map of all synthesized materials, confirming near-complete β coverage within a given E_0 range (Figure 4C). The map yields several notable correlations highlighted by dashed cross-sectional lines: (i) Horizontal cross section I represents collections of plastomers with constant E_0 and increasing β similar to those found in Figure 4A as achieved by larger $\langle n_{sc} \rangle$. (ii) Two vertical cross sections II and III correspond to plastomers with constant β and variable E_0 realized by concomitantly varying ϕ_L and $\langle n_{sc} \rangle$ (Figure 4B). (iii) Diagonal dashed lines correspond to plastomers with a given $\langle n_{sc} \rangle$ (series 1–9 in Table 1), where increasing ϕ_L simultaneously increases E_0 and β up the coalesced line, which can be exploited to fill the elastic landscape with samples of higher E_0 beyond the reported samples with small ϕ_L . These correlations enable general design rules toward architecturally traversing the $[E_0, \beta]$ landscape. Further theoretical analysis discussed in the literature^{6,36} allows collapsing the individual series trends into distinct correlations for bottlebrushes and combs (Figure 4D), which demonstrates overarching universality by correlating the attained mechanical properties (E_0, β) with their corresponding architectural parameters ($n_{bb}, n_{sc}, n_L, \phi_L$). The observed collapse underlines the general physical nature of the plastomer elasticity and cross-correlation between softness (E_0) and firmness (β). However, trendline boundaries are currently ill-defined as there could be a

change in microdomain symmetry upon reaching high ϕ_L ,³⁷ which will be a topic of future study.

Further demonstrating the adaptability of the side chain mixing approach, we deliberately introduce heterogeneous distribution of side chains with different n_{sc} along the brush backbone. To this end, we have synthesized two pentablock copolymers $\text{LB}_{14}\text{B}_{71}\text{B}_{14}\text{L}$ and $\text{LB}_{71}\text{B}_{14}\text{B}_{71}\text{L}$, where B_{14} and B_{71} correspond of monodisperse blocks with $n_{sc} = 14$ or $n_{sc} = 71$ side chains, respectively (Figures S21 and S22). The two brush triblocks ($\text{B}_{14}\text{B}_{71}\text{B}_{14}$ and $\text{B}_{71}\text{B}_{14}\text{B}_{71}$) with inverted side chains distributions were grown to have similar $\langle n_{sc} \rangle \cong 47$ (Table S6), which is analogous to series 7 in Table 1. The stress–elongation curves (Figure 4E) of these blocky plastomers show slightly lower β from series 7 obtained with random copolymerization (Figure 4F). Although each pentablock differs in ϕ_L and n_{bb} (Table S6), their similar $\langle n_{sc} \rangle$ enables their coalesced trendline that is remarkably comparable to the randomly copolymerized LBL's. This observation suggests that the LBL plastomer footprint on the $[E_0, \beta]$ landscape is largely $\langle n_{sc} \rangle$ controlled; however, the precise effect of side chain distribution within a given brush strand will be investigated in future studies.

CONCLUSION

In conclusion, self-assembly of linear–brush–linear macromolecules yields physical networks that can span the entire elastic landscape via their architectural multiplet $[n_{bb}, n_{sc1}, n_{sc2}, n_L, \phi_L, m_1]$, where m_1 is the molar fraction of side chain with $\text{DP} = n_{sc1}$. Specifically, the side chain mixing approach allows covering the entire firmness range at a given Young's modulus to replicate the elastic properties of both synthetic gels and biological tissue. Thus, the average side chain length $\langle n_{sc} \rangle$ is the defining architectural feature that enables encoding elastomers with unique pairings of both softness and firmness that have eluded polymer science and have stalled many relevant fields. Therefore, we believe this industrially friendly platform will revolutionize future applications pertinent to the established fields of dielectric elastomers, adhesives, vibration control, wearable electronics, tissue engineering, biomedical implants, and soft robotics.

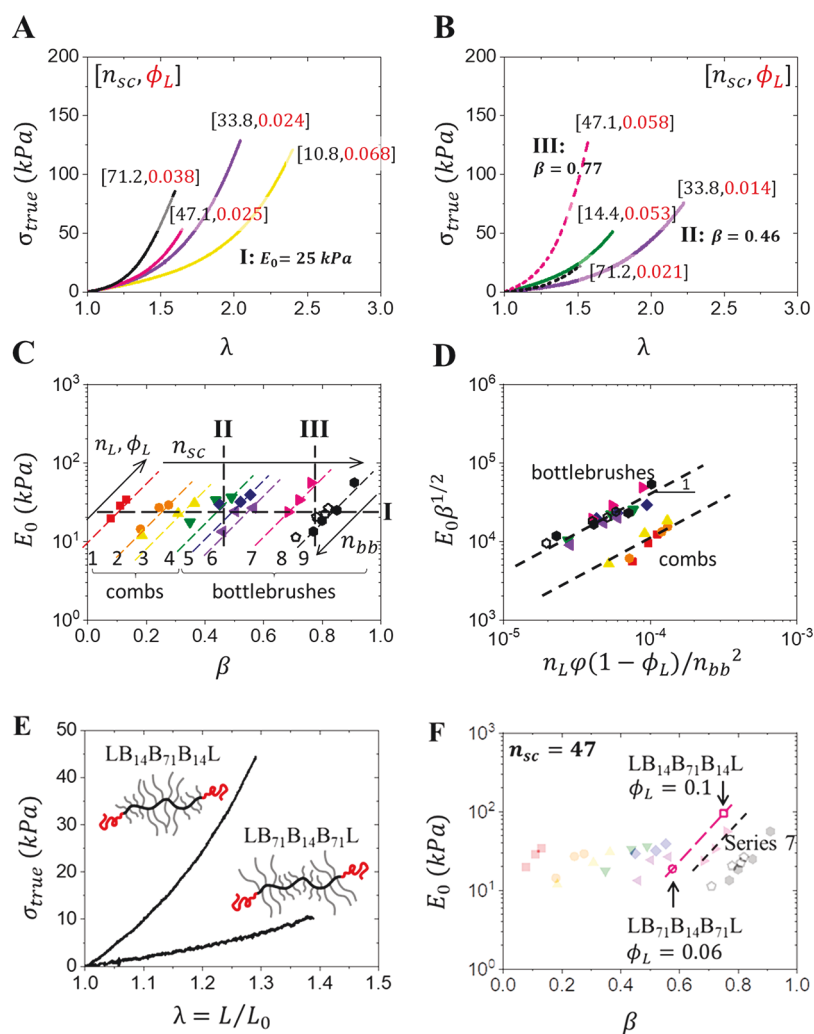


Figure 4. Mechanical characterization. (A) Stress–elongation curves of selected LBL plastomers with similar $E_0 = 25$ kPa and different β . (B) Stress–elongation curves of LBL plastomers of two groups (dashed vs solid line) with similar $\beta = 0.77$ and $\beta = 0.46$ but different E_0 . (C) Elastic parameters of reported LBL plastomers extracted from a collection of stress–elongation curves (Figure S20) on an $[E_0, \beta]$ map. Each colored symbol set represents a series according to Table 1. Dashed lines are provided to guide the reader and delineate the coalescence of each series. Collections of stress–elongation with either constant E_0 and different β (A) or constant β and different E_0 (B) may be identified by respectively dropping lateral lines (I) or vertical lines (II,III). General design rules (arrows) can be inferred for tuning mechanical properties (E_0, β) with architectural parameters ($n_{bb}, n_{sc}, n_L, \phi_L$). (D) Universal collapse of attained mechanical properties in relation to their programmed architectural parameters informed by previously reported theoretical analysis^{6,36} provides a direct route for programmable design, where $\varphi = n_g/(n_g + n_{sc})$ corresponds to the volume fraction of the backbone in the brush block and n_g is the degree of polymerization of the backbone spacer between neighboring side chains ($n_g = 1$ for the bottlebrushes and $1 < n_g < 2$ for the combs). Both bottlebrushes and combs exhibit distinct coalescence due to their fundamental difference in their effective Kuhn length.³⁸ (E) Stress–elongation curve profiles of $LB_{14}B_{71}B_{14}L$ and $LB_{71}B_{14}B_{71}L$ pentablock plastomers. (F) $LB_{14}B_{71}B_{14}L$ and $LB_{71}B_{14}B_{71}L$ pentablock plastomers on the elastic map programmed with $\langle n_{sc} \rangle$ similar to series 7. The observed shift is likely due to small errors in determining $\langle n_{sc} \rangle$ of randomly mixed brushes (Figures S6 and S7).

■ ASSOCIATED CONTENT

Supporting Information

The Supporting Information is available free of charge at <https://pubs.acs.org/doi/10.1021/acs.macromol.0c01725>.

Synthetic procedures with 1H NMR and sample summaries, atomic force microscopy, and mechanical characterization with stress–elongation curves of triblock and pentablock plastomers with mixed side chains (PDF)

■ AUTHOR INFORMATION

Corresponding Authors

Sergei S. Sheiko – Department of Chemistry, University of North Carolina at Chapel Hill, Chapel Hill, North Carolina 27599,

United States; orcid.org/0000-0003-3672-1611;

Email: sergei@email.unc.edu

Andrey V. Dobrynin – Department of Chemistry, University of North Carolina at Chapel Hill, Chapel Hill, North Carolina 27599, United States; orcid.org/0000-0002-6484-7409;
Email: avd@email.unc.edu

Authors

Andrew N. Keith – Department of Chemistry, University of North Carolina at Chapel Hill, Chapel Hill, North Carolina 27599, United States; orcid.org/0000-0001-6351-5392

Charles Clair – Laboratoire de Physique et Mécanique Textiles, Université de Haute Alsace, F-68093 Cedex Mulhouse, France

Abdelaziz Lallam — Laboratoire de Physique et Mécanique Textiles, Université de Haute Alsace, F-68093 Cedex Mulhouse, France

Egor A. Bersenev — Lomonosov Moscow State University, 119991 Moscow, Russian Federation; Institute of Problems of Chemical Physics, Russian Academy of Sciences, Chernogolovka 142432, Russian Federation

Dimitri A. Ivanov — CNRS UMR 7361, Institut de Sciences des Matériaux de Mulhouse-IS2M, F-68057 Mulhouse, France; Lomonosov Moscow State University, 119991 Moscow, Russian Federation; Institute of Problems of Chemical Physics, Russian Academy of Sciences, Chernogolovka 142432, Russian Federation; orcid.org/0000-0002-5905-2652

Yuan Tian — Department of Chemistry, University of North Carolina at Chapel Hill, Chapel Hill, North Carolina 27599, United States; orcid.org/0000-0002-7277-1408

Complete contact information is available at:

<https://pubs.acs.org/10.1021/acs.macromol.0c01725>

Author Contributions

A.N.K. designed, synthesized, and characterized the monomers, block copolymers, and polymer networks. A.N.K. performed mechanical tests and AFM experiments. Y.T. and A.V.D. provided theoretical analysis of mechanical properties and developed theoretical foundation for materials design and LBL networks. C.C., A.L., E.B., and D.A.I. conducted X-ray studies and data analysis. S.S.S. is the principal investigator and corresponding author. A.N.K. and S.S.S. were primary writers of the manuscript. All authors discussed the results and provided feedback on the manuscript.

Notes

The authors declare no competing financial interest.

ACKNOWLEDGMENTS

We acknowledge funding from the National Science Foundation (DMR 1921835, DMR 1921923, and DMR 2004048). D.A.I. and E.B. acknowledge the Ministry of Science and Higher Education of Russian Federation for financial support in the frame of project RFME-19X0100, N 075-15-2019-1889 from December 5, 2019. The work was done in the frame of state task No. 0074-2019-0014 (registration no. AAAA-A19-119101590029-0). The authors acknowledge perfect technical support of the personnel of the ID02 beamline of the European Synchrotron Radiation Facility (ESRF) in Grenoble, France.

REFERENCES

- (1) Dobrynin, A. V.; Carrillo, J. Y. Universality in Nonlinear Elasticity of Biological and Polymeric Networks and Gels. *Macromolecules* **2011**, *44*, 140–146.
- (2) Carrillo, J.-M. Y.; MacKintosh, F. C.; Dobrynin, A. V. Nonlinear Elasticity: from Single Chain to Networks and Gels. *Macromolecules* **2013**, *46*, 3679–3692.
- (3) Kraft, E. Varying firmness mattress. U.S. Patent US513674 0A, 1996.
- (4) Juarez, B.; King, J. J.; Bachlava, E.; Wentzell, A. M.; Mills, J. M. Methods and Compositions for Watermelon Firmness. U.S. Patent US10036032 B2, 2012.
- (5) Brown, T.; Brown, S.; Murphy, T. Breast Durometer (mammometer): A Novel Device for Measuring Soft-Tissue Firmness and its Application in Cosmetic Breast Surgery. *Aesthetic. Plast. Surg.* **2017**, *41*, 265–274.
- (6) Keith, A. N.; Vatanikhah-Varnosfaderani, M.; Clair, C.; Fahimipour, F.; Dashtimoghdam, E.; Lallam, A.; Sztucki, M.; Ivanov,

- D. A.; Liang, H.; Dobrynin, A. V.; Sheiko, S. S. Bottlebrush Bridge between Soft Gels and Firm Tissues. *ACS Cent. Sci.* **2020**, *6*, 413–419.
- (7) Blair, G. W. S. A New Criterion for Expressing the 'Intensity of Firmness' of Soft Bodies. *Nature* **1943**, *152*, 412.
- (8) Faber, T. J.; Jaishankar, A.; McKinley, G. H. Describing the Firmness, Springiness and Rubberiness of Food Gels Using Fractional Calculus. Part I: Theoretical framework. *Food Hydrocolloids* **2017**, *62*, 311–324.
- (9) Sheiko, S. S.; Dobrynin, A. V. Architectural Code for Rubber Elasticity: from Super-Soft to Super-Firm Materials. *Macromolecules* **2019**, *52*, 7531–7546.
- (10) Daniel, W. F. M.; Burdyńska, J.; Vatanikhah-Varnosfaderani, M.; Matyjaszewski, K.; Paturej, J.; Rubinstein, M.; Dobrynin, A. V.; Sheiko, S. S. Solvent-Free, Supersoft and Superelastic Bottlebrush Melts and Networks. *Nat. Mater.* **2016**, *15*, 183.
- (11) Jacobs, M.; Liang, H.; Dashtimoghdam, E.; Morgan, B. J.; Sheiko, S. S.; Dobrynin, A. V. Nonlinear Elasticity and Swelling of Comb and Bottlebrush Networks. *Macromolecules* **2019**, *52*, 5095–5101.
- (12) Gong, J. P.; Katsuyama, Y.; Kurokawa, T.; Osada, Y. Double-Network Hydrogels with Extremely High Mechanical Strength. *Adv. Mater.* **2003**, *15*, 1155–1158.
- (13) Ducrot, E.; Chen, Y.; Bulters, M.; Sijbesma, R. P.; Creton, C. Toughening Elastomers with Sacrificial Bonds and Watching them Break. *Science* **2014**, *344*, 186–189.
- (14) Storm, C.; Pastore, J. J.; MacKintosh, F. C.; Lubensky, T. C.; Janmey, P. A. Nonlinear Elasticity in Biological Gels. *Nature* **2005**, *435*, 191–194.
- (15) Fung, Y. C. *Biomechanics: Mechanical Properties of Living Tissues*; Springer: 1993.
- (16) Holzapfel, G. A. Biomechanics of soft tissue. In *Handbook of Material Behavior Models*; Lemaitre, J., Ed.; Academic Press: 2001; pp 1057–1071.
- (17) Vatanikhah-Varnosfaderani, M.; Daniel, W. F. M.; Everhart, M. H.; Pandya, A. A.; Liang, H.; Matyjaszewski, K.; Dobrynin, A. V.; Sheiko, S. S. Mimicking Biological Stress-Strain Behavior with Synthetic Elastomers. *Nature* **2017**, *549*, 497–501.
- (18) Vatanikhah-Varnosfaderani, M.; Daniel, W. F. M.; Zhushma, A. P.; Li, Q.; Morgan, B. J.; Matyjaszewski, K.; Armstrong, D. P.; Spontak, R. J.; Dobrynin, A. V.; Sheiko, S. S. Bottlebrush Elastomers: A New Platform for Freestanding Electroactuation. *Adv. Mater.* **2017**, *29*, 1604209.
- (19) Pakula, T.; Zhang, Y.; Matyjaszewski, K.; Lee, H.-i.; Boerner, H.; Qin, S.; Berry, G. C. Molecular brushes as Super-soft elastomers. *Polymer* **2006**, *47*, 7198–7206.
- (20) Sheiko, S. S.; Sumerlin, B. S.; Matyjaszewski, K. Cylindrical Molecular Brushes: Synthesis, Characterization, and Properties. *Prog. Polym. Sci.* **2008**, *33*, 759–785.
- (21) Verduzco, R.; Li, X.; Pesek, S. L.; Stein, G. E. Structure, Function, Self-Assembly, and Applications of Bottlebrush Copolymers. *Chem. Soc. Rev.* **2015**, *44*, 2405–2420.
- (22) Reynolds, V. G.; Mukherjee, S.; Xie, R.; Levi, A. E.; Atassi, A.; Uchiyama, T.; Wang, H.; Chabiny, M. L.; Bates, C. M. Super-Soft Solvent-Free Bottlebrush Elastomers for Touch Sensing. *Mater. Horiz.* **2020**, *7*, 181–187.
- (23) Sarapas, J. M.; Chan, E. P.; Rettner, E. M.; Beers, K. L. Compressing and Swelling to Study the Structure of Extremely Soft Bottlebrush Networks Prepared by ROMP. *Macromolecules* **2018**, *51*, 2359–2366.
- (24) Liberman-Martin, A. L.; Chu, C. K.; Grubbs, R. H. Application of Bottlebrush Block Copolymers as Photonic Crystals. *Macromol. Rapid Commun.* **2017**, *38*, 1700058.
- (25) Bolton, J.; Rzaev, J. Synthesis and Melt Self-Assembly of PS-PMMA-PLA Triblock Bottlebrush Copolymers. *Macromolecules* **2014**, *47*, 2864–2874.
- (26) Dalsin, S. J.; Rions-Maehren, T. G.; Beam, M. D.; Bates, F. S.; Hillmyer, M. A.; Matsen, M. W. Bottlebrush Block Polymers: Quantitative Theory and Experiments. *ACS Nano* **2015**, *9*, 12233–12245.

- (27) Vatankeh-Varnosfaderani, M.; Keith, A. N.; Cong, Y.; Liang, H.; Rosenthal, M.; Sztucki, M.; Clair, C.; Magonov, S.; Ivanov, D. A.; Dobrynin, A. V.; Sheiko, S. S. Chameleon-like Elastomers with Molecularly Encoded Strain-Adaptive Stiffening and Coloration. *Science* **2018**, 359, 1509–1513.
- (28) Clair, C.; Lallam, A.; Rosenthal, M.; Sztucki, M.; Vatankeh-Varnosfaderani, M.; Keith, A. N.; Cong, Y.; Liang, H.; Dobrynin, A. V.; Sheiko, S. S.; Ivanov, D. A. Strained Bottlebrushes in Super-Soft Physical Networks. *ACS Macro Lett.* **2019**, 8, 530–534.
- (29) Cong, Y.; Vatankeh-Varnosfaderani, M.; Karimkhani, V.; Keith, A. N.; Leibfarth, F.; Martinez, M.; Matyjaszewski, K.; Sheiko, S. S. Understanding the synthesis of linear-bottlebrush-linear block copolymers: towards elastomers with well-defined mechanical properties. *Macromolecules* **2020**, 53, 8324.
- (30) Burdyska, J.; Daniel, W.; Li, Y.; Robertson, B.; Sheiko, S. S.; Matyjaszewski, K. Molecular Bottlebrushes with Bimodal Length Distribution of Side Chains. *Macromolecules* **2015**, 48, 4813–4822.
- (31) Pakula, T.; Minkin, P.; L. Beers, K.; Matyjaszewski, K. Structure and Dynamics in Melts of Bottle-Brush Polymers. *Polym. Mater.: Sci. Eng.* **2001**, 84, 1006–1007.
- (32) López-Barron, C. R.; Tsou, A. H.; Younker, J. M.; Norman, A. I.; Schaefer, J. J.; Hagadorn, J. R.; Throckmorton, J. A. Microstructure of Crystallizable α -Olefin Molecular Bottlebrushes: Isotactic and Atactic Poly(1-octadecene). *Macromolecules* **2018**, 51, 872–883.
- (33) Sarapas, J. M.; Martin, T. B.; Chremos, A.; Douglas, J. F.; Beers, K. L. Bottlebrush Polymers in the Melt and Polyelectrolytes in Solution Share Common Structural Features. *Proc. Natl. Acad. Sci. U. S. A.* **2020**, 117, 5168–5175.
- (34) Liang, H.; Wang, Z.; Dobrynin, A. V. Scattering from Melts of Combs and Bottlebrushes: Molecular Dynamics Simulations and Theoretical Study. *Macromolecules* **2019**, 52, 5555–5562.
- (35) Sheiko, S. S.; Sun, F. C.; Randall, A.; Shirvanyants, D.; Rubinstein, M.; Lee, H.; Matyjaszewski, K. Adsorption-induced scission of carbon-carbon bonds. *Nature* **2006**, 440, 191–194.
- (36) Liang, H.; Wang, Z.; Dobrynin, A. V. Strain-Adaptive Self-Assembled Networks of Linear-Bottlebrush-Linear Copolymers. *Macromolecules* **2019**, 52, 8617–8624.
- (37) Zhulina, E. B.; Sheiko, S. S.; Dobrynin, A. V.; Borisov, O. V. Microphase Segregation in the Melts of Bottlebrush Block Copolymers. *Macromolecules* **2020**, 53, 2582–2593.
- (38) Liang, H.; Morgan, B. J.; Xie, G.; Martinez, M.; Zhulina, E. B.; Matyjaszewski, K.; Sheiko, S. S.; Dobrynin, A. V. Universality of the Entanglement Plateau Modulus of Comb and Bottlebrush Polymer Melts. *Macromolecules* **2018**, 51, 10028–10039.